



Highlights of the 35th EANM Annual Congress 2022, onsite edition in Barcelona, Spain: “FROM BARCELONA WITH LOVE”

Nathalie L. Albert¹ · Philippe Garrigue² · Benjamin Guillet² · Irene A. Burger^{3,4}

Published online: 11 July 2023
© The Author(s) 2023

Keywords EANM2022 · Annual Congress · Abstracts · Nuclear medicine · Highlight · Top oral presentations

Introduction

The 35th Annual Congress of the European Association of Nuclear Medicine (EANM) took place in Barcelona, Spain, between the 15th and 19th October 2022. After two virtual editions due to the SARS-CoV-2 pandemic, organizers and participants were excited to finally have a real “face-to-face” meeting again and made this conference, under the chairmanship of Professor Fanti, an unforgettable event.

With 7233 on-site registrations from 121 different countries, EANM’22 even increased the number of total participants compared to 2019 (6955 registrations). Despite the high on-site attendance, the online access was still intensively used. A total of 1980 min of live-streamed content reached more than 150,000 hits on the virtual platform during the congress days. Afterwards, the congress offered two additional months of on-demand access for selected sessions (including the possibility to collect CME credits).

Out of 1881 submitted abstracts from 71 different countries, 1563 were accepted with 603 abstracts considered for oral presentations and 195 rated as potential highlights by the reviewers of the respective subcommittees. This year, Spain was the most productive country (11.3%), followed by

Italy (10.4%) and Germany (6.8%). A very remarkable effort came from India, ranking on the fourth place with 5.8% of all submitted abstracts (Fig. 1).

The congress program offered scientific sessions, numerous joint symposia including specialists from other societies, and a variety of invited speakers’ lectures such as plenary lectures, CME sessions, LIPS session, special sessions and a broad range of abstract sessions covering all relevant fields of nuclear medicine.

This review gives a summary of our personal choice among the most notable scientific abstract contributions of this year’s conference, presented in the Highlights Lecture of the Annual congress of the EANM’22.

Neurology highlights

In the neurology section, numerous abstracts were rated as potential highlights. The topics covered encompassed neurodegenerative diseases, neuroinflammation as well as neuro-oncology.

Recent longitudinal tau positron emission tomography (PET) studies indicated that global amyloid is associated with greater tau spreading. Yet, the role of regional amyloid in this regard is still limited. Hoenig et al. examined the contribution of regional amyloid load to longitudinal tau spreading using a data-driven approach of parallel independent component analysis (pICA) on PET data [1] (OP120). They found baseline amyloid load in specific brain regions to be associated with tau increase in different brain regions, leading to the hypothesis that regional amyloid may be the initiator of tau increases in early Braak stages, but not the direct facilitator of tau spread to advanced Braak stages. Peretti et al. investigated the prognostic value of ATN profiles in a memory clinic cohort [1] (OP134). In this study, 154 patients from the

✉ Irene A. Burger
Irene.burger@usz.ch

¹ Department of Nuclear Medicine, University Hospital, LMU Munich, Munich, Germany

² Aix-Marseille Univ, APHM, C2VN, CERIMED, INSERM, INRAE, CNRS, Radiopharmacy, Marseille, France

³ Department of Nuclear Medicine, Kantonsspital Baden, Baden, Switzerland

⁴ Department of Nuclear Medicine, University Hospital Zürich, University of Zürich, Rämistrasse 100, 8091 Zürich, Switzerland

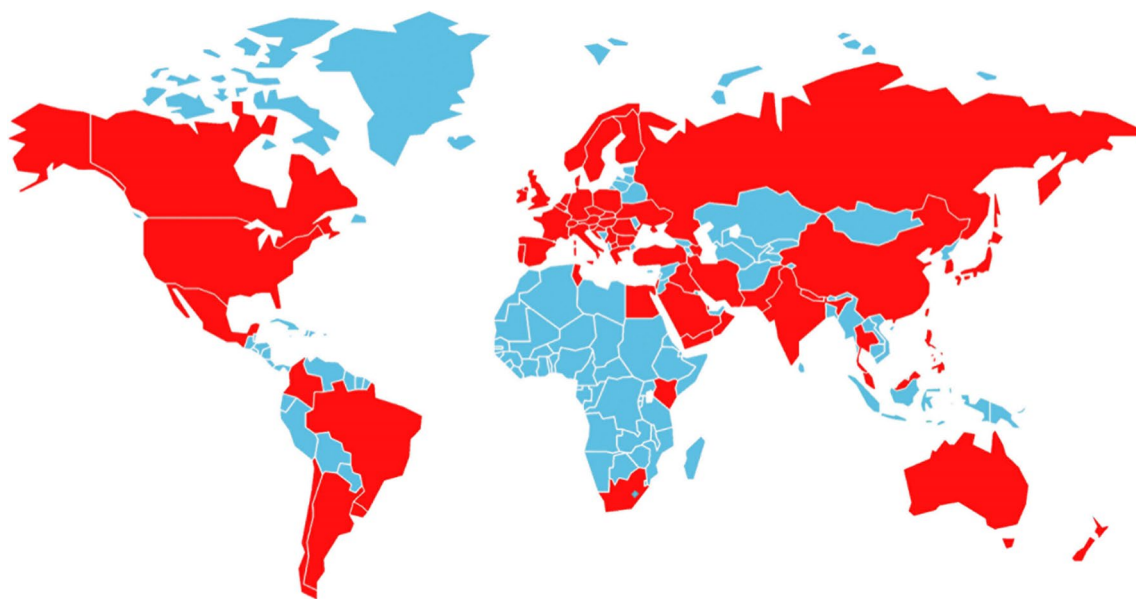


Fig. 1 Countries with abstract contributions for EANM 2022 (red)

Memory Clinic of Geneva were analyzed, and the ATN profiles were correlated to their clinical state at baseline and after 2 years. They found that tau positivity had the most significant effect on cognitive decline over a period of 2 years, highlighting the value of molecular imaging as a prognostic biomarker in clinical practice. Instead of using real follow-up data such as in the former study, a collaborative study from Shanghai and Bern used a machine learning–based algorithm for disease progression modeling in patients with progressive supranuclear palsy (PSP) [1] (OP548). The aim was to subtype and stage PSP on tau PET, which is of particular interest as sequential distribution patterns of PSP pathology had been described *in vitro*, but not yet *in vivo*. In their study with 148 PSP patients and 20 healthy controls, the machine learning technique “SuStaIn” was applied to perform clustering with disease progression modeling and identified two subtypes of PSP: subtype 1 showed sequential progression from subcortical to cortical regions with slow spread from region to region, but fast spread within the same structure. Subtype 2, by contrast, showed fast spread from region to region with simultaneous involvement of subcortical and cortical regions. These findings were consistent with pathological findings of heterogeneity of PSP tau suggesting similar initiating sites, but different propagation patterns. In another study by the same group, deep learning has been applied to improve the clinical interpretation of TAU PET imaging [1] (OP129). The authors trained a Convolutional Neural Network (CNN) on [^{18}F]florbetapir PET images to classify Alzheimer’s disease (AD), PSP, and controls in two different cohorts, one with magnetic resonance

imaging (MRI) available and one without MRI. The deep learning classifier outperformed semiquantitative analyses in disease identification, and was comparably high using MR-free approaches, so that deep learning serves as classifier for TAU PET image interpretation even in the absence of MR images.

Importantly, the neurology highlights did not only cover neurodegenerative diseases: Cheval et al. evaluated patients with drug-resistant focal epilepsy and compared translocator protein (TSPO) PET imaging to conventional [^{18}F]FDG PET for pre-surgical localization of the epileptogenic zone [1] (OP319). TSPO PET was significantly better than [^{18}F]FDG PET in detecting abnormalities, with more than 95% of patients showing an abnormality on TSPO PET, while only half were abnormal on [^{18}F]FDG PET. This was even feasible by simple visual analysis. Therefore, TSPO PET appears to be a promising diagnostic tool for the localization of the epileptogenic focus (see Fig. 2).

Another neurology project focused on stem cell tracking in patients with traumatic spinal cord injury, for whom stem cell therapy has emerged as a promising treatment strategy. Jug et al. investigated stem cell kinetics and retention at the site of injury by labeling mesenchymal stem cells in 9 patients with spinal cord injury [1] (OP769). They labeled autologous mesenchymal stem cells with [$^{99\text{m}}\text{Tc}$]HMPAO which were transplanted intrathecally by lumbar puncture and imaged 1, 4, and 24 h p.i. Tracer signal could be found in all but one patient at the site of injury, and it will be interesting to correlate the signal intensity to the clinical outcome in future analyses.

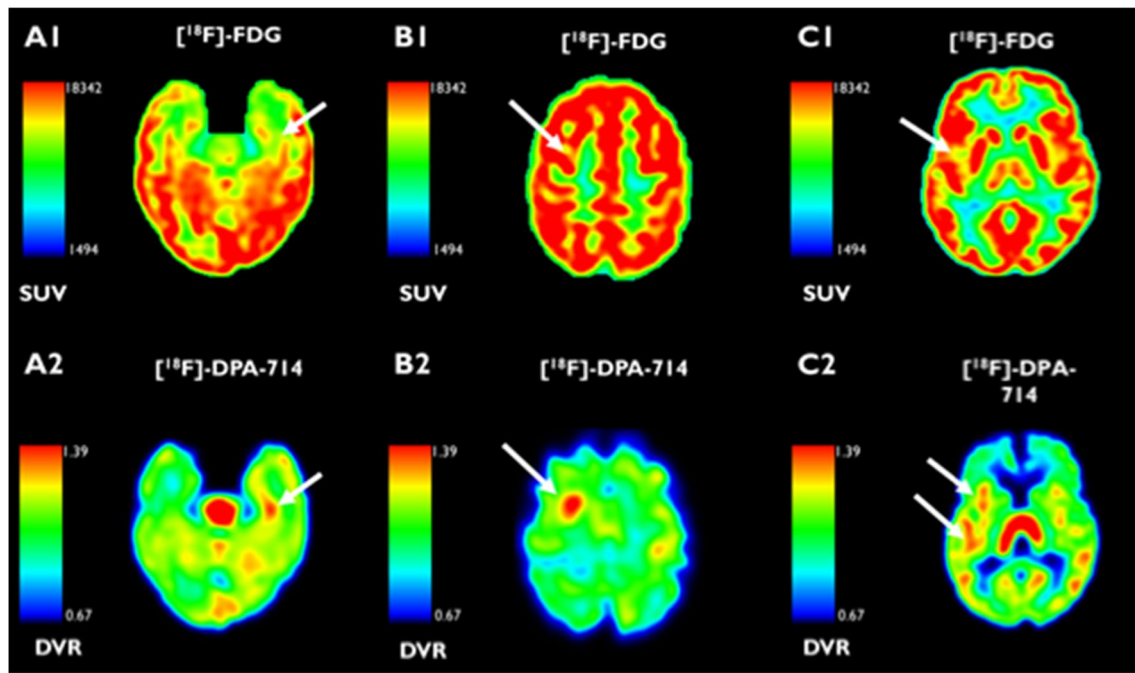


Fig. 2 **A** Patient with left temporal suspected EZ; **B** patient with right pericentral suspected EZ; **C** patient with right insular suspected EZ; EZ, epileptogenic zone (with courtesy from Cheval et al.)

Also neuro-oncological topics showed interesting highlights: Fiz et al. [1] (OP202) presented a prospective study with 10 pediatric patients with diffuse high-grade gliomas (PDHGG) or diffuse intrinsic pontine gliomas (DIPG), who received $^{64}\text{CuCl}_2$. $^{64}\text{CuCl}_2$ is a positron- and Auger electron emitter which may represent a novel diagnostic and theranostic tool in brain tumor patients. After i.v. injection of $^{64}\text{CuCl}_2$, uptake was found in areas with contrast enhancement on MRI, and constant tracer accumulation was found up to 3 days after injection, which seems promising for possible theranostic applications. Another interesting neuro-oncological study which may be of relevance for future therapeutic applications was presented by Pruis et al. from Rotterdam [1] (OP253). They introduced the principle of theranostics and intra-arterial (IA) administration of radionuclides to the field of neuro-oncology in order to improve current and explore novel treatment strategies. Patients with meningioma, brain metastases, or glioblastoma received PET/CT scans after intravenous and separate intraarterial administration through selective catheterization of a tumor-feeding artery) of either ^{68}Ga]Ga-DOTATATE or ^{68}Ga]Ga-PSMA-11. Intraarterial administration of radionuclides led to a strong, significant and relevant increase in tumor uptake, which may open new avenues for the development of more effective theranostic strategies, which are desperately needed for patients with CNS tumors.

Technical, dosimetry, and AI highlights

There were 16 abstracts rated as potential highlights in the very active fields of technical developments, dosimetry, and artificial intelligence for this year's conference.

Mingels et al. studied the clinical impact of ultra-high sensitivity mode in comparison to the currently available high sensitivity mode in long axial PET scanner [1] (OP236). Thirty-eight patients were analyzed in a LAFOV PET/CT, using newly available ultra-high sensitivity (UHS) mode compared to the routinely used high sensitivity (HS) mode with ^{18}F]F-FDG, ^{18}F]F-PSMA-1007, and ^{68}Ga]Ga-DOTA-TOC. UHS enabled higher signal-to-noise ratios irrespective of the radiotracer, significantly improved the image quality with smaller bias for SUV_{max} measurement, and an acquisition shortened to 20 s–2 min. UHS may have an advantage in the conspicuity of tumor lesions and in scanning children or patients in pain.

Krarp et al. reported the evaluation of ultra-low dose PET/CT efficiency using LAFOV PET [1] (OP235). Five oncological patients successively underwent ultra-low dose PET/CT and a full dose PET/CT. By increasing the duration of acquisition, the image quality of ultra-low dose PET was at least comparable to the current clinical standard, but with a total radiation dose of only 1 mSv approximately. Delgado Cano et al. reported their experience with a new brain-dedicated PET scanner [1] (OP607).

In a completely different context, dosimetry for peptide receptor radiotherapy is a broad active research field and the team of Chicheportiche et al. developed and validated a multiple linear regression model for dosimetry of PRRT based on a single scan [1] (EP492). They previously trained the multiple linear regression model based on 40 multiple time-points SPECT/CT studies. Then, out of a test set of more than 200 patients and more than 600 PRRT cycles with multiple time-points dosimetry, they could show a very high agreement between regular dosimetry results compared to the dose estimations from a single post PRRT SPECT/CT study regarding cumulative absorbed doses especially in kidney, bone marrow, liver, spleen, and tumor lesions.

Kryzaniak et al. introduced the concept of dosimetry planning in SIRT with the help of a 360° CZT camera [1] (OP822). Three different phantoms of different volumes were used to determine calibration factors and mean dose recovery coefficients (mDRC) in a VERITON-CT camera. The influence of SPECT acquisition time reduction on mDRC values was also studied. The absolute quantification error was less than 1% whatever the phantoms. The reconstruction parameters had no influence on mDRC for the largest volumes, but there was a variation for the smaller spheres. The authors concluded on the reliable dosimetric SIRT planning using this 360° CZT camera for a lesion bigger than 8 mL, in less than a 10-min acquisition. Doyen et al. evaluated the association between [¹⁸F]FDG metabolic connectivity and post temporal lobe epilepsy surgery patient outcome [1] (OP306). Voxel-to-voxel group analysis did not differentiate patient outcome, however, metabolic connectivity analysis performed with two complementary methods successfully predicted surgery patient outcome.

Sundar et al. led a multi-organ, whole body PET-driven systemic analysis for early stratification of lung cancer patients with or without cachexia, as 60% of lung cancer patients actually develop cachexia, with poor prognosis [1] (OP679). Whole-body PET data of 77 non-cachectic and 80 cachectic lung cancer patients were analyzed through the 3-step ENHANCE-PET framework. Disparities between correlation patterns were observed in both groups in subcutaneous fat and the psoas muscle, hinting towards a possible metabolic fingerprint which might be unique to cachexia.

A critical bottleneck for AI-based methods is their limited capability in the heterogeneous domain of PET imaging, due to the variety of scanners and tracers. Xue et al. developed a simple way to integrate domain knowledge in deep learning for CT-free PET imaging [1] (OP242). In contrast to conventional direct deep learning methods, they decomposed the complex end-to-end generation into anatomy-independent textures (relating to tracers and diseases) and anatomy-dependent correction.

The efficiency and robustness were verified in tests with more than 800 patients, fluoride-18 and gallium-68

imaging tracers, 4 different commercial scanners. This method improved the performance and robustness of CT-free PET correction. Ochoa Figuerola et al. evaluated a deep learning attenuation correction software (DLACS) in the performance of myocardial perfusion imaging using a cardiology-dedicated CZT camera, with invasive coronary angiography correlation for the diagnosis of coronary artery disease in a high-risk population [1] (OP397).

To build more accurate prognostic models for patients with metastatic non-small cell lung cancer treated with immunotherapy in first or second lines, Schmutz et al. used machine learning algorithms to combine clinical, biological, and PET/CT parameters [1] (OP751). A dataset of 117 patients was analyzed through a total of 28 clinical, biological, and PET/CT features. The clinical endpoint to train the prognostic model was the progression-free survival at 6 months and the overall survival at 12 months. Features were sorted according to their selection frequency using a LASSO logistic regression and an exhaustive cross-validation. The model performances were analyzed using either the top 4 features, the top 8 features, or all of the 28 features. For both outcomes, the models using the top 4 or the top 8 features outperformed the model using all the 28 features without selection, as well as the simple baseline with no biomarker. This work underlined the interest of combining clinical, biological, and imaging biomarkers for predicting the outcome, but also the importance in rigorously selecting the features to improve model performances.

Oncology highlights — license to detect cancer

The most relevant newcomers in diagnostic oncology this year were the inhibiting molecules for the fibroblast activation protein (FAP), a target that is overexpressed in cancer-associated fibroblasts of several tumor entities. With only a few submitted abstracts in 2021, FAPI ($n=20$) surpassed PSMA ($n=19$) this year as a target among the highly rated abstracts. This underlines how incredibly dynamic the field is moving forward.

Novruzov et al. from Azerbaijan presented data from 100 patients with primary breast cancer imaged with [⁶⁸Ga]Ga-FAPI-46 and [¹⁸F]FDG PET/CT. Patients were scanned after 10, 30, and 60 min. A significant increase in tumor to background ratio was seen from 10 to 30 min followed by a plateau phase; therefore, 30-min uptake time might be sufficient for adequate imaging. In both the primary tumors as well as axillary lymph nodes, FAPI uptake was significantly higher compared to FDG. Given the generally low liver uptake, a lesion to liver ratio was even more in favor for [⁶⁸Ga]Ga-FAPI-46 PET [1] (OP351). Dr. Backhaus et al. from Münster, Germany, presented a first insight into FAPI PET for

the assessment of therapy response. They imaged 13 women before and after neoadjuvant chemotherapy and compared the accuracy of MRI and [^{68}Ga]Ga-FAPI-46 PET to predict complete pathologic response based on the resected specimens. Visual analysis as well as a tumor to background (contralateral breast) ratio < 1.0 could predict complete pathologic response in all 13 women, while MRI was false negative in 2 and false positive in one case [1] (OP348).

The largest study for [^{68}Ga]Ga-FAPI-46 PET was presented by Dr. Fendler et al. from Essen, Germany. A large multicenter cohort including 324 patients with 21 different tumor entities imaged between 2018 and 2021 were collected. Seventy-three percent of the patients had a simultaneous [^{18}F]FDG PET. The authors could show that the tumor to liver ratio is higher for FAPI compared to FDG in all solid tumors. Intense [^{68}Ga]Ga-FAPI-46 accumulation was observed in sarcomas, pancreatic cancer, mesothelioma, and cholangiocellular carcinoma [1] (OP354) (Fig. 3).

For prostate cancer imaging using the prostate specific membrane antigen (PSMA), also interesting novel aspects were presented. With the new possibilities of the novel long axial field of view PET scanners, a protocol to combine [^{68}Ga]Ga-PSMA-11 with [^{18}F]F-FDG within a 2-h protocol was proposed by Schepers et al. from Bern, Switzerland. After injection of a regular dose of [^{68}Ga]Ga-PSMA-11 a 5-min scan was performed after 60 min, followed by an injection of 40 MBq [^{18}F]F-FDG and a second scan for 15 min 1 h later. Subtraction of scan 1 from scan 2 would show miss match lesions and offer an elegant way to do therapy selection in a one-stop-shop approach [1] (OP338). With the presentation of the PYTHON trial Dr. Rischpler et al. presented the results of a multicentric prospective trial

investigating the accuracy of [^{18}F]F-DCFPyL-PET to detect biochemical recurrence after primary therapy with curative intent. The results in 205 patients showed that [^{18}F]F-DCFPyL-PET was safe, and superior to [^{18}F]F-Fluorocholine-PET for the detection of biochemical recurrence for all PSA levels [1] (OP153). The use of [^{18}F] instead of [^{68}Ga] offers various advantages regarding logistics and costs. Therefore, also [^{18}F]-labeled ligands targeting the SSTR were proposed. Unterrainer et al. from Munich, Germany, proposed the use of [^{18}F]F-SiTATE to improve image quality for meningioma and received the EANM Young Authors Award for his work [1] (OP543). Finally, the Marie Curie Award was given to Dr. Pauwels et al. from Leuven, Belgium, for the presentation of their [^{18}F]AIF-NOTA-octreotide vs. [^{68}Ga]Ga-DOTA-somatostatin analogue PET. They could show that the mean detection ratio for the [^{18}F]AIF compound was not only non-inferior but even superior compared to [^{68}Ga]Ga-DOTATATE [1] (OP544) (Fig. 4).

Preclinical highlights and radiopharmaceutical developments

There were 18 abstracts rated as potential highlights in pre-clinical and radiopharmaceutical developments, showing that innovative concepts for constant improving of targeting and efficacy for imaging and radioligand therapy are at the core of nuclear medicine.

Among the multiple innovative targets for molecular imaging and theranostics in oncology, the CD70-CD27 axis is involved as an immune checkpoint especially in hematological and solid malignancies. Elvas et al. reported

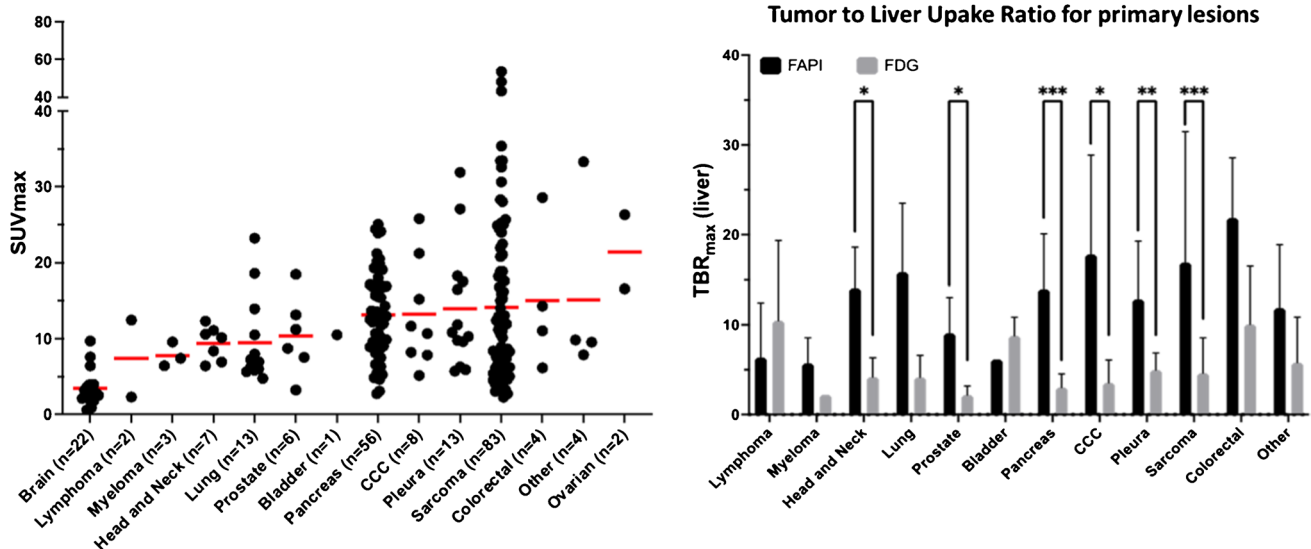


Fig. 3 **A** [^{68}Ga]Ga-FAPI-46 PET uptake (SUVmax) in a variety of different tumor entities. **B** Tumor to liver ratios for FAPI in comparison to FDG for different tumor entities (with courtesy from Dr. W. Fendler) [2]

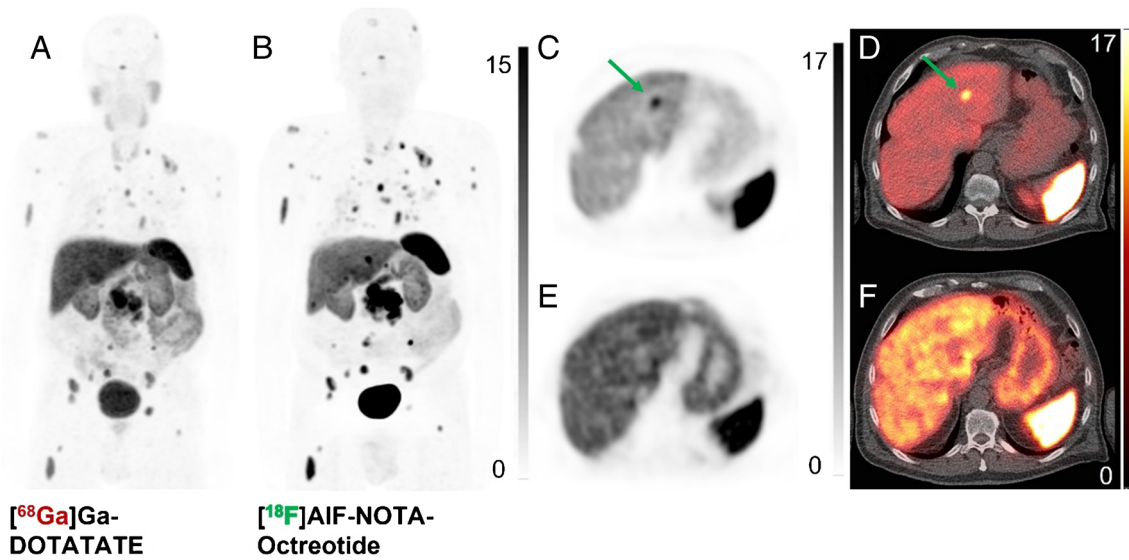


Fig. 4 Maximum intensity projection (MIP) images of $[^{68}\text{Ga}]\text{Ga-DOTATATE}$ (A) and $[^{18}\text{F}]\text{AlF-NOTA-Octreotide}$ (B) PET/CT images acquired in a 55-year-old male patient with a pancreatic NET, revealing 60 and 88 NET lesions, respectively (images scaled to same SUV, color bar denotes range of lookup table). Transverse slices highlight lower background in the liver in the $[^{18}\text{F}]\text{AlF-NOTA-Octreotide}$ (native PET: C; PET/CT fusion: D), allowing detection of an incremental lesion (green arrows), not depicted on the corresponding $[^{68}\text{Ga}]\text{Ga-DOTATATE}$ slices (native PET: E; PET/CT fusion: F). This highlights one of the advantages of $[^{18}\text{F}]\text{AlF-NOTA-Octreotide}$, lower liver background allowing depiction of liver metastases missed on $[^{68}\text{Ga}]\text{Ga-DOTATATE}$. Other advantages include higher production yields allowing more patients to be scanned per batch, transport to distant PET centers and longer injection-scan interval with increased tumor-to-background ratio (OP544). (With courtesy from Dr. C. Deroose and Dr. E. Pauwel)

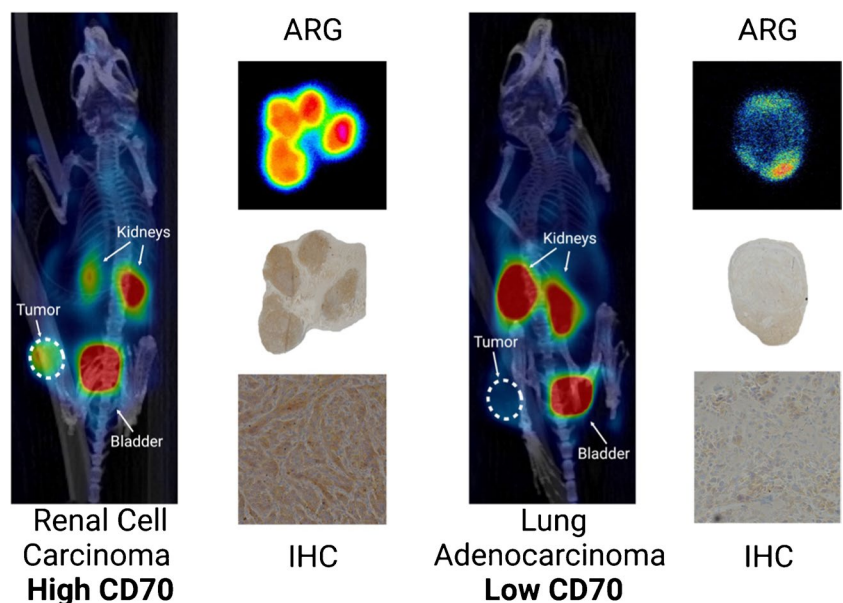
Other advantages include higher production yields allowing more patients to be scanned per batch, transport to distant PET centers and longer injection-scan interval with increased tumor-to-background ratio (OP544). (With courtesy from Dr. C. Deroose and Dr. E. Pauwel)

a gallium-68-radiolabelled single domain antibody fragment targeting CD70 developed for immunoPET imaging and aiming at defining patient eligibility to CD70 targeted therapies [1] (OP877). The radiotracer showed fast clearance from the blood, CD70 specificity was verified in two CD70 high-expressing cells lines ($\text{CD70}^{\text{high}}$) and affinity was evaluated at the nanomolar range. In xenografted nude mice, an

intense PET signal was found in $\text{CD70}^{\text{high}}$ tumors compared to low CD70^{low} tumors, as confirmed per autoradiography and consistently with CD70 immunohistochemistry (Fig. 5).

Novel targets were also reported for neurology, as Jie et al. evaluated the interest of a novel molecular target for imaging Alzheimer’s disease [1] (OP557). Aside from the amyloid plaque and tau tangles, the mitochondrial

Fig. 5 Representative PET imaging, autoradiography (ARG) and immunohistochemistry (IHC) samples of CD70 high-expressing renal cell carcinoma xenografts and CD70 low-expressing lung adenocarcinoma xenografts in nude mice injected with a gallium-68-radiolabelled single domain antibody fragment targeting CD70 (OP877)



dysfunction recently raised the interest of the scientific community in Alzheimer's disease, and especially regarding an actor of the electron transport chain. The alpha subunit of ATP synthase, also known as ATP5A, was reported as decreased in AD post-mortem brains. The authors developed carbon-11 radiolabeled J147, a reported ATP5A compound. Using autoradiography, a 20% reduction in ATP5A was found in two different rodent models of AD. Preliminary in vivo PET imaging in healthy rats showed high brain uptake of the radiotracer. The authors intend to test this in an AD rat model compared to [^{18}F] F-FDG in the near future. According to the hypothesis that the soluble form of A β oligomers accumulate many years before clinical AD symptoms and its predictive value of memory decline, Dumulon-Perreault et al. developed an innovative radiotracer that specifically targets the soluble form of A β oligomers but not the deposit [1] (OP558). Thus, copper-64–radiolabeled anti-amyloidogenic azapeptides were radiosynthesized and evaluated in two clinically relevant transgenic murine models of Alzheimer's disease. A significant PET signal was found in the thalamus in 44-day-old 5XFAD mice, and even more intense on day 72, exhibiting unprecedented early detection ability of A β oligomer formation. Interestingly, the PET signal was significantly more intense than that of the [^{11}C]C-Pittsburg compound B on day 95.

With the aim to improve target-to-background or healthy tissue signals on common molecular targets, many strategies were highlighted this year. To decrease kidney exposure and off-target nephrotoxicity, Poty et al. evaluated the interest of a two-step pretargeted approach using the trans-cyclooctene/tetrazine couple [1] (OP878). Applied to FAP targeting in a subcutaneous glioblastoma murine model, the injection of an anti-FAP, trans-cyclooctene-functionalized single domain antibody, followed by the injection of lutetium-177 radiolabeled tetrazin, resulted in a significant sevenfold decrease in kidney exposure and a fivefold increase in tumor-to-kidney ratio. Another reported strategy was to increase the residence time of the radiotracer in the blood compartment by adding a DOTA-conjugated albumin binding domain on DARPin G3, a HER2 targeting moiety [1] (OP093). After radiolabeling with lutetium-177 and injection in mice bearing HER2-positive SKOV3 tumors, the significant extension of the radiotracer half-life in blood was associated with a decrease of the SPECT signals in the liver and in the kidneys, and a sixfold increase in tumor signal at 48-h post-injection. Originally, Mansi et al. explored the possibility of enhancing mIBG uptake in neuroendocrine tumors via pharmacological upregulation of norepinephrine transporters (NET) [1] (OP165). The authors screened several inhibitors of the histone deacetylase and the PI3K/AKT/mTOR pathway. The lead inhibitor compound significantly increased the internalization of [^{123}I]–mIBG in

neuroblastoma cells via upregulation of NET expression. In an in vivo proof of concept study in IGR-NB8 xenografts, the pretreatment with the inhibitor did not affect the total body distribution of [^{123}I]–mIBG but doubled the tumor uptake, holding promises for the improvement of the efficacy of [^{131}I]–mIBG therapy.

Aiming at better understanding the cellular effects of alpha therapy, Hernandez et al. stated that immunological effects drove efficacy differences of alpha- versus beta- radioligand therapy in prostate cancer [1] (OP620). The NM600 compound was radiolabeled either with lutetium-177 or actinium-225 and further injected to a syngeneic murine prostate cancer model. [^{177}Lu]Lu-NM600 led to modest tumor growth inhibition with no survival benefit, whereas [^{225}Ac]Ac-NM600 treatment resulted in both tumor growth inhibition and extended survival at low injected activities, all treatments being well tolerated. Afterwards, the tumor tissues were collected and submitted to flow cytometry, highlighting [^{225}Ac]Ac-NM600 but not [^{177}Lu]Lu-NM600 depleted immunosuppressive cell lineages such as Treg lymphocytes and myeloid-derived suppressor cells on day 28. Overall, [^{225}Ac]Ac-NM600 showed a distinctive pro-inflammatory profile in the tumor microenvironment of prostate cancer model, with interesting potential as single agent and in combination with immunotherapy for mCRPC.

This year, the preclinical highlights also included original technical developments for radiotracer screening and development. Löffler et al. notably demonstrated the feasibility of a chorioallantoic-membrane (CAM) model as an alternative to mouse model for in ovo inhibition studies of novel radiotracers, using [^{18}F]F-siPSMA-14 and the corresponding inhibitor 2-PMPA [1] (EP047). After establishing tumor xenografts of PSMA-positive (LNCaP) and PSMA-negative (PC-3) cell lines on the CAM, various concentrations of a PSMA-inhibitor were administered 20 min before the injection of [^{18}F]F-siPSMA-14 to the CAM. Only a weak PET signal could be detected in PSMA-positive tumors pre-dosed with the highest inhibitor concentration, while a pronounced accumulation of the PET tracer was observed in absence of inhibitor. In contrast, no PET tracer accumulation was observed in PSMA-negative tumors. The team concluded that the CAM model had a great potential as an alternative to mouse models for receptor-specific radiotracer binding studies, as a cost-effective and easily applicable method and in terms of the 3Rs principles.

Bartos et al. reported a novel method called “single-cell radiotracing” for cell specific analysis of radiotracers uptake [1] (OP367). Combining radiotracers exposure, cell sorting with magnetic antibodies, flow cytometry, and gamma counter, tumors cells were isolated from immune cells, and their respective activity was counted, enabling

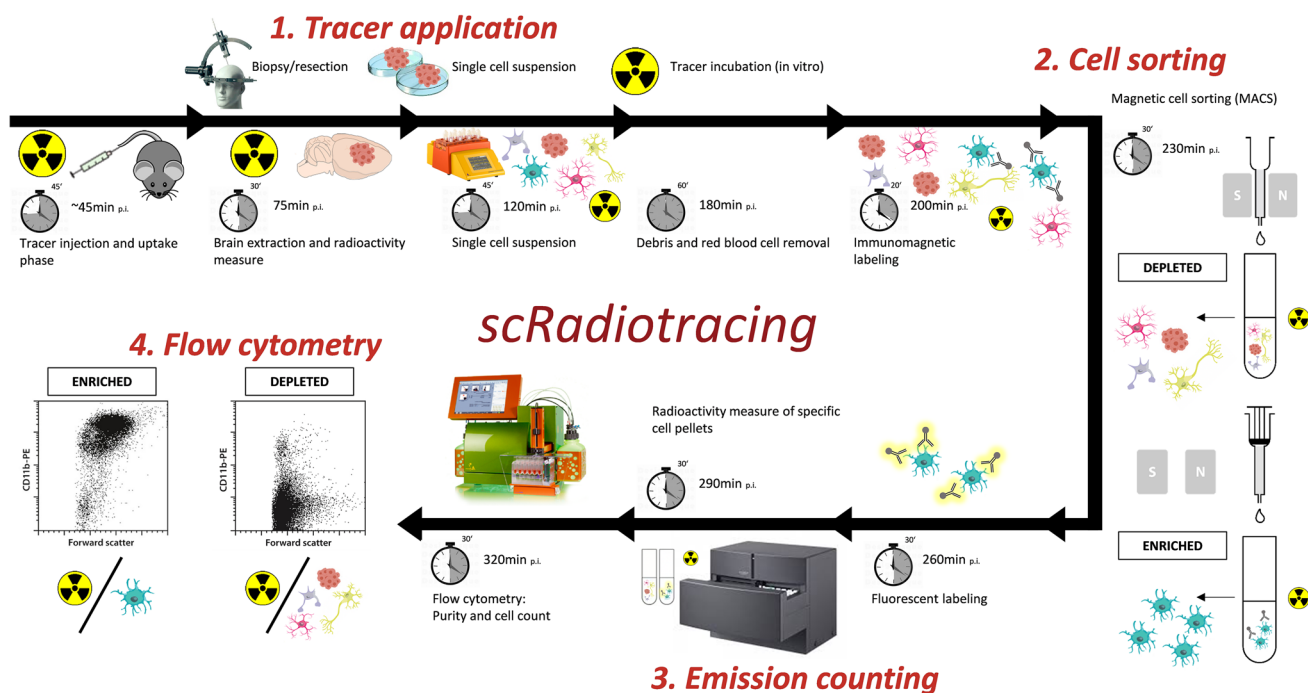


Fig. 6 “Single-cell Radiotracing” for analysis of cell type specific radiotracer uptake, applied to a glioblastoma model in mice after in vivo injection of a TSPO ligand and to human glioblastoma tissues after in vitro TSPO PET radiotracer incubation (OP367)

radiotracer uptake quantification according to cell types in heterogenous tissues. Applied to a glioblastoma model in mice and to human glioblastoma tissues ex vivo submitted to TSPO PET radiotracers, they surprisingly observed that the radiotracer uptake was more intense in tumor cells than in immune cells, and significantly more elevated in single tumor cells of high-grade glioma compared to low-grade glioma patients (Fig. 6).

Oncology highlights — license to kill cancer...

LaFrance et al. presented the interim results of the ongoing ReSPECT-GBM Phase I/IIa trial for recurrent glioblastoma patients, in whom Rhenium-186 encapsulated naoliposomes are delivered to the tumor via convection enhanced delivery [1] (OP542). So far, they included 23 patients with increasing therapy doses. Notably, a significant overall survival benefit was found for patients with > 100 Gy tumor absorbed radiation dose compared to those with < 100 Gy. Importantly, no dose-limiting toxicities have been observed pre-clinically or clinically, showing that the treatment is safe and well-tolerated, with limited and minor adverse events. These results are highly encouraging and underpin the potential of radionuclide therapies as treatment option in patients with CNS tumors.

An important and still unmet clinical need are patients with iodine refractory thyroid cancer. Kersting et al. presented the results from a single center Phase II trial including patients with radioiodine refractory follicular thyroid carcinomas who were treated according to their BRAF mutation status either with a MEK inhibitor alone (Trametinib; BRAF wild-type patients) or a combination of MEK- and BRAF-inhibition (Dabrafenib; BRAF mutant patients) [1] (OP698). ^{124}I -PET/CT was performed before and after 3 weeks regimen for redifferentiation. In both groups, about one-third of the patients showed adequate redifferentiation, suggesting that the addition of dabrafenib worked sufficiently. In another single-center prospective phase 0 study, eight patients with advanced medullary thyroid carcinoma were investigated after administration of [^{177}Lu]Lu-PP-F11N, a cholecystokinin 2 receptor agonist, with and without pretreatment using the neutral endopeptidase-1 inhibitor sacubitril [1] (OP700). Indeed, enzymatic blocking increased the stability of the compound in the blood and consequently improved tumor uptake of [^{177}Lu]Lu-PP-F11N.

Also this year therapeutic highlights for prostate cancer and neuroendocrine tumors (NET) were presented. Dr Hermann, Essen, Germany, presented the health-related quality of life outcomes of the VISION study, the last year presented phase 3 trial for [^{177}Lu]Lu-PSMA-617 in patients with metastatic castration-resistant prostate cancer. Despite discussions

that the exclusion of taxane-based therapy was a limitation of the study, the presented data showed significantly longer time to worsening in the FACT-P score (a combination of physical, social and emotional well-being) as well as the pain intensity score. Concluding that, the efficacy of [^{177}Lu]Lu-PSMA-617 in prolonging OS and rPFS in patients with mCRPC was associated with a longer period without deterioration in patient-reported HRQoL and pain vs. SoC alone, as well as a delay in time to first SSE or death [1] (OP161).

With the results from the OCLURANDOM trial Dr. Baudin et al., Villejuif, France, presented the first randomized phase II study for metastatic pancreatic NET. The study met its primary endpoint of achieving significantly longer progression-free survival (PFS) with a 12-month PFS rates of 80.5% with [^{177}Lu]Lu-DOTATATE (33/41 patients; 90% confidence interval [CI] 67.5–89.9) versus 42% with sunitinib (18/43 patients; 90% CI 29.1–55.5) [1] (OP154). This study closes an important gap since pancreatic NET was not covered in the NETTER trial. Further improvement in NET therapy might be achieved with the use of an alpha emitting nuclide. Dr. Tworowska et al. from Houston, USA, presented data using [^{212}Pb]Pb-DOTAMATE in patients that were progressive after regular PRRT. In this prospective phase I study, they included 10 patients that received up to four, 8-week cycles of [^{212}Pb]Pb-DOTAMATE. Response to treatment was measured per RECIST 1.1 with [^{68}Ga]Ga- or [^{64}Cu]Cu-DOTATATE PET/CT. In 7 of 10 patients, partial response could be observed.

Finally, the use of FAP as a target for therapy was also present at EANM 2022. Of four abstracts suggested as highlights, we selected two, prospective multicenter studies: a basket phase 1/2 study including patients with advanced or metastatic solid tumors, the LuMIERE trial and a study focusing on solitary fibrous tumors.

Dr. T. Hope et al. CA, USA, presented the multicenter LuMIERE data evaluating the safety and tolerability of [^{177}Lu]Lu-FAP-2286. Patients with advanced solid tumors with three or more therapy lines were selected and planar and SPECT/CT scans performed at 4, 24, 48, and 168 h after each dose in each cycle to calculate organ and tumor dosimetry. The recruiting included already dose levels from 3.7 to 7.4 GBq. In this range, the safety profile was manageable, and some preliminary antitumor activity could be observed [1] (OP355). The second abstract presented by Dr. Fendler et al. Essen, Germany, focused on the use of FAP as a theranostic target in solitary fibrous tumors (SFT). The work was based on an extensive immunohistochemistry and immunofluorescence study on a pan cancer cohort with over 800 patients and 126 tumor

entities. They identified solitary fibrous tumors as the tumor type with the highest FAP expression and went on with a prospective imaging study with 38 patients that confirmed high or intermediate expression in 66% of the patients. Resulting in higher accumulation on [^{68}Ga]Ga-FAPI-46 PET compared to [^{18}F]F-FDG in 12 patients. Seven patients subsequently underwent RLT and were treated with [^{90}Y]Y-FAPI-46. Disease control was reached in all cases, two had a partial response, and the median PFS was 266 days [1] (OP356).

Acknowledgements We greatly acknowledge all authors for their availability to simplify and share their work and send us slides and videos of their abstracts in time. We furthermore thank the EANM staff for their valuable support in the preparation of the EANM 2022 Highlights Lecture, in particular Susanne Koebe.

Declarations

Ethics approval This article does not contain any studies with human participants or animals performed by any of the authors.

Informed consent Not applicable.

Competing interests IAB has received research grants and speaker honorarium from GE Healthcare, research grants from Swiss Life, and speaker honorarium from Bayer Health Care and Astellas Pharma AG. NLA has received honoraria as consultant and advisory board member from Novartis and Telix and research grants from Novocure. BG has received honoraria as consultant from Novartis.

Open Access This article is licensed under a Creative Commons Attribution 4.0 International License, which permits use, sharing, adaptation, distribution and reproduction in any medium or format, as long as you give appropriate credit to the original author(s) and the source, provide a link to the Creative Commons licence, and indicate if changes were made. The images or other third party material in this article are included in the article's Creative Commons licence, unless indicated otherwise in a credit line to the material. If material is not included in the article's Creative Commons licence and your intended use is not permitted by statutory regulation or exceeds the permitted use, you will need to obtain permission directly from the copyright holder. To view a copy of this licence, visit <http://creativecommons.org/licenses/by/4.0/>.

References

1. Annual Congress of the European Association of Nuclear Medicine October 15–19, 2022 Barcelona, Spain. *Eur J Nucl Med Mol Imaging.* 2022;49(1): 1–751. <https://doi.org/10.1007/s00259-022-05924-4>.
2. Hirmas N, Hamacher R, Sraieb M, Ingenwerth M, Kessler L, Pabst KM, et al. Fibroblast-activation protein PET and histopathology in a single-center database of 324 patients and 21 tumor entities. *J Nucl Med.* 2023;64:711–6. <https://doi.org/10.2967/jnumed.122.264689>.

Publisher's note Springer Nature remains neutral with regard to jurisdictional claims in published maps and institutional affiliations.